Chemical Engineering Science, Vol. 49, No. 2, pp. 171–178, 1994.
Printed in Great Britain.

0009-2509/94 $6.00 + 0.00

CROSS-FLOW FILTRATION WITH AND WITHOUT CAKE FORMATION

M. R. MACKLEY and N. E. SHERMAN†
Department of Chemical Engineering, University of Cambridge, Pembroke Street, Cambridge CB2 3RA, U.K.

Abstract—A neutrally buoyant model particulate suspension has been used to examine the effect of channel flow fluid mechanics on filtrate flux kinetics. The incorporation of periodically spaced central baffles is shown to improve filtration performance by a factor of about two. Direct observations of particle activity at the cake surface show that this improvement is caused by filter cake erosion due to eddy circulation around the baffles. A novel piece of apparatus has been developed to produce oscillatory flow within the channel. When these oscillations were superimposed upon a steady net flow in the presence of baffles, more than tenfold filtrate flux enhancement was found. Optical observations of the filtration process show that in this mode of operation, cake build up is completely inhibited. It was also observed that more efficient filtration occurs when gas was entrained into the channel, through the filter.

INTRODUCTION

Pressure-driven filtration has been widely studied in recent years and much effort placed on the understanding of the processes which limit performance, namely concentration polarisation [e.g. Porter, (1972a, b)], fouling [e.g. Aimar *et al.* (1991) and Jonsson *et al.* (1992)] and filter cake formation [e.g. Fordham and Ladva (1989); Mackley and Sherman (1992); Pearson and Sherwood (1988)], which in some cases is combined with the mechanism of pore blocking of the filter (Jonsson *et al.*, 1992). In many cases, the rationale behind the investigation of these processes is that, by understanding the mechanisms by which limitation occurs, it may become possible to inhibit or even prevent them and consequently enhance filtrate yields.

A simple method of cake growth or polarisation layer limitation is to operate at a high cross-flow velocity. However, this usually requires repeated suspension recirculation with any given volume making many passes through the filter cell. Also, it has been found that higher cross-flows may not necessarily lead to higher fluxes [e.g. Lu and Ju (1989); Mackley and Sherman (1992) and Wakeman and Tarleton (1991a)] due to the selective infiltration of fines and more efficient particle packing. Clearly then, it is desirable to limit rejected phase build-up without resorting to high-level recirculation in order to increase the net separation per unit length of filter and unsteady laminar flows would appear to offer a suitable method.

In a recent review, Winzler and Belfort (1993) have shown that a large number of workers in the field of cross-flow filtration are utilising unsteadiness in cross-flow to try to enhance filtrate flux. They classified the methods for generating instabilities as (1) roughness—where protuberances are placed on or close to the membrane/filter surface, (2) pulsation—where oscillations are superimposed onto a steady net flow, and (3) secondary flows—where filter cell geometry is chosen in order that instabilities such as Taylor or Dean vortices are generated. Winzler and Belfort comment that simultaneous use of more than one of these methods had also been successfully employed. Of particular interest in the context of this paper is the combination of oscillatory flow and sharp edge baffle inserts. Finnigan and Howell (1989) found that, by incorporating periodically spaced baffles at the wall of a tubular ultrafiltration membrane module and superimposing oscillations at a frequency of ~ 2 Hz onto a net cross-flow of Reynolds number $Re_n \sim 570$–1710, an approximately fourfold flux enhancement could be obtained. Similar levels of enhancement were also found by Coleman and Mitchell (1991) working under similar oscillatory conditions with centrally placed baffles.

Alternatively to intrinsic flow instabilities, other workers have employed periodic back-washing of the filter/membrane in order to remove rejected phase deposits. Nakao *et al.* (1990) demonstrated that for the filtration of submicron PMMA particles, repeated back-washing with the filtrate could produce time-averaged fluxes a factor of three higher than the equivalent steady cross-flow steady-state fluxes. Further, Peters and Pedersen (1992) obtained a 50% increase in flux by applying a periodic gas back-flush during wine filtration.

Although for the purposes of this work our interest lies in fluid instabilities and gas back-flow, it should be noted that another class of deposition inhibiting method exists based around the application of steady or unsteady external fields. Examples include the electrophoretic method described by Lentsch *et al.* (1992) and the electroacoustic cross-flow microfiltration technique of Wakeman and Tarleton (1991b). These have been shown to produce flux enhancement in

†Present address: DRA, Farnborough, Hants GU14 6TD, U.K. Author to whom correspondence should be addressed.

macromolecular and particulate systems, respectively.

In this paper we present a method which combines the elements of roughness, pulsation and back-flush to produce a scheme whereby filter cake build-up is prevented. Consequently, high filtrate flux is maintained and the effect of long-term flux decline is substantially reduced.

EXPERIMENTAL

A model suspension of neutrally buoyant polyethylene particles, having diameter in the range 125–180 μm, dispersed in a Newtonian liquid comprising water and methylated spirit (viscosity = 2.38 mPa s at 22°C) was prepared at a solids volume concentration of 0.1%. This suspension was chosen as it has been found to be useful for flow visualisation studies. Although the particle size is somewhat large compared with, e.g. typical microfiltration operation, their behaviour has been observed to be representative of particles of size up to that where Brownian effects become important. For example, the reduction in filtrate flux with increasing cross flow velocity found for these particles (reported in Mackley and Sherman, 1992) has also been observed by Wakeman and Tarleton (1991a) for ~ 25 μm calcite particles.

The experimental filtration rig used for this suspension has been described in more detail previously [see Mackley and Sherman (1992)]. A schematic diagram of the apparatus used is reproduced here in Fig. 1(a). The essential features were that (i) the flow channel allowed direct observation of the volume above the filter and facilitated cake height measurements, (ii) simultaneously with cake height measurements, filtrate flux was continuously monitored, (iii) the filtration could be conducted under constant differential pressure conditions of 5 kPa, being much greater than the pressure drop along the filter channel, i.e. ~ 0.1 kPa, (iv) an optical resolution of ~ 100 μm was achieved such that individual particles could be readily observed.

This filtration cell was connected via the ports shown in Fig. 1(a) to a device which enabled oscillation of the fluid in the flow cell; this apparatus is shown in Fig. 1(b). An electronically controlled variable speed motor was used to drive a crank and piston arrangement. Both frequency and amplitude of stroke could be varied in the range 0–10 Hz and 0–15 mm, respectively. The piston was connected to a plate which separated the chambers of the two bellows assemblies [as shown in Fig. 1(b)] and was used to expand and contract them in antiphase, i.e. as the plate moved from left to right, bellows chamber 1 was expanded, drawing in fluid through exit 1, and chamber 2 was contracted pushing fluid out from exit 2; the roles were reversed on the return stroke. Hence, by continuously running the motor at a given frequency, oscillations could be superimposed on the net fluid flow in the test cell.

Another feature of the apparatus used was the inclusion of centrally placed baffles, as shown in Fig. 2. Central baffles were chosen as these had previously

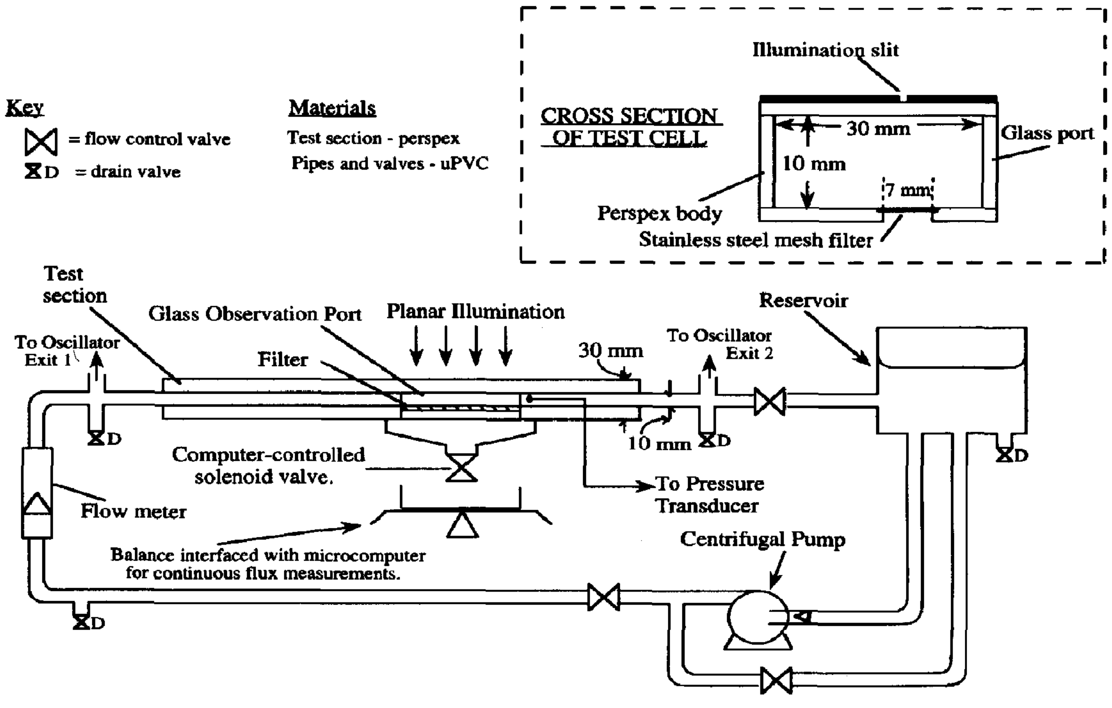

Fig. 1(a). Schematic diagram of the flow loop and test cell.

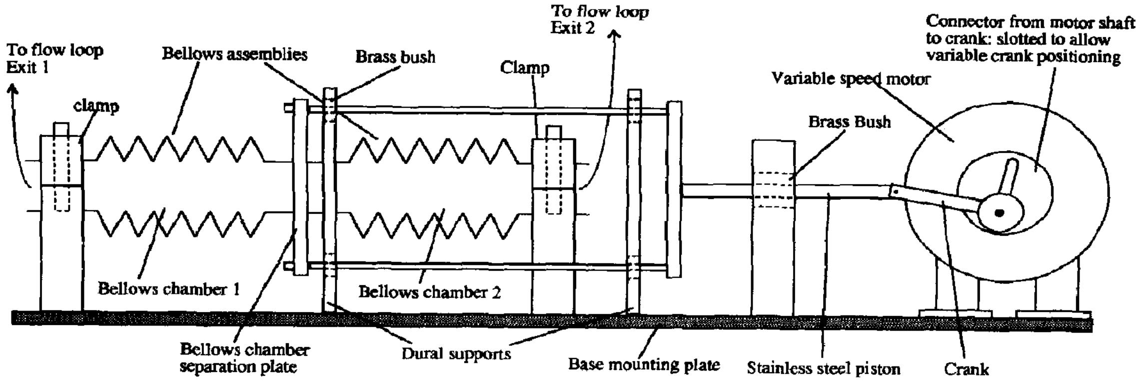

Fig. 1(b). Schematic diagram of oscillating bellows assembly.

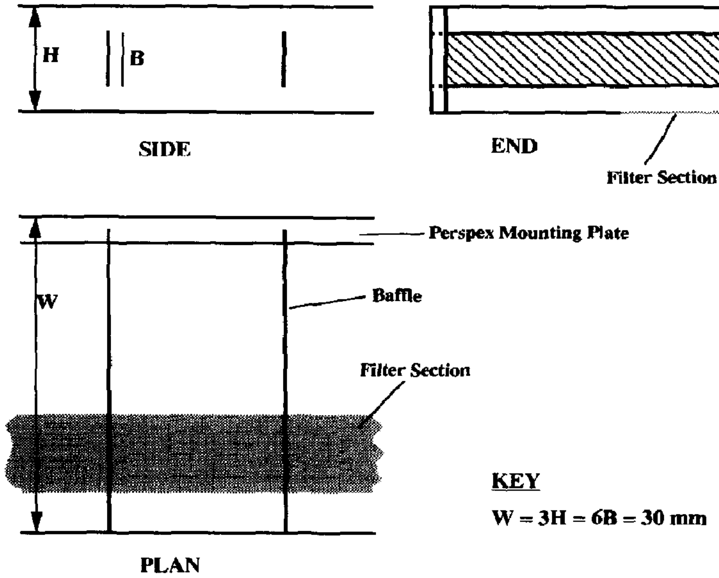

Fig. 2. Schematic diagram of the baffled channel.

been found to provide more efficient filter cake erosion (cf. wall baffles) [see Mackley and Sherman (1993)]. The baffles were chosen for near-optimum inter-baffle fluid mixing with an area constriction of 50% and spacing of 1.5 times the channel height, as found by Brunold *et al.* (1989) using flow visualisation techniques. The baffles extended across the whole width of the channel and were supported in a Perspex mounting plate, which was push-fitted into the cell. The perspex plate did represent a narrowing of the channel width (i.e. 3 mm in 30 mm) but was not found to disturb the flow patterns above the filter. The baffle configuration used here is similar to that tested by Coleman and Mitchell (1991).

Using the above apparatus, the model suspension was filtered under various oscillatory flow conditions at constant mean differential pressure $\Delta P = 5$ kPa and constant net flow Reynolds number $Re_n = 450$, where

$$Re_n = \frac{(\bar{v}H\rho)}{\eta}$$

and $\bar{v}$ is the mean cross-flow velocity, H is the channel height and ρ, η are the fluid density and viscosity, respectively. In this case $\rho = 940$ kg/m^3 and $\eta = 2.38$ mPa s.

The oscillatory flows can be characterised in terms of an oscillatory Reynolds number,

$$Re_0 = \frac{(\omega x_0 H\rho)}{\eta}$$

and the Strouhal number,

$$St = \frac{H}{(2\pi x_0)}$$

where ω is the angular frequency of oscillation and x_0

is the centre to peak amplitude of oscillation. In the experiments reported here x_0 was set at 5 mm (i.e. 10 mm total stroke). This was chosen to produce eddies of order one half the inter-baffle spacing in size (determined by flow visualisation) on both the forward and reverse stroke, thus providing good mixing in the whole inter-baffle volume in one cycle. Thus, when oscillations were applied, the Strouhal number was fixed at $St = 0.32$. Experiments were conducted at frequencies of 0, 5 and 10 Hz corresponding to $Re_0 = 0$, 640 and 1280. Also the effect of the inclusion of baffles and the re-entrainment of liquid or gas through the filter during the filtration cycle were investigated.

RESULTS AND DISCUSSION

Steady flow

Filtrate flux kinetics. The data obtained for filtrate flux as a function of time under steady cross-flow conditions are shown in Fig. 3. The flux exhibits an initial rapid decline followed by a slower long-term decrease. It can be seen that the effect of the inclusion of baffles is to increase the long-term flux from about 0.75×10^{-3} to $\sim 2.25 \times 10^{-3}$ m/s giving a three-fold increase, comparable with the findings of Finnigan and Howell (1989) for a wall baffled tubular membrane module. However, in both cases shown in Fig. 3, the long-term flux is still approximately a factor of ten down on that obtained initially.

Cake formation. The case of unbaffled steady flow, filter cake formation has been studied and is described elsewhere (Mackley and Sherman, 1992). For the purpose of this work, it is sufficient to say that the filtrate flux decline is caused by the build-up on the filter of a layer of particles, the height of which grows with time. A schematic diagram of the type of long-term cake formed in these experiments is given in Fig. 4. The cakes appear to be of uniform thickness along the filter, apart from small development regions at the entry and exit.

In the case where baffles are present, the cake formation is significantly perturbed and Fig. 5 shows a flow visualisation time sequence for cake evolution. Frame 5(a) shows the fluid mechanics above the filter before filtration commences. Flow is from left to right

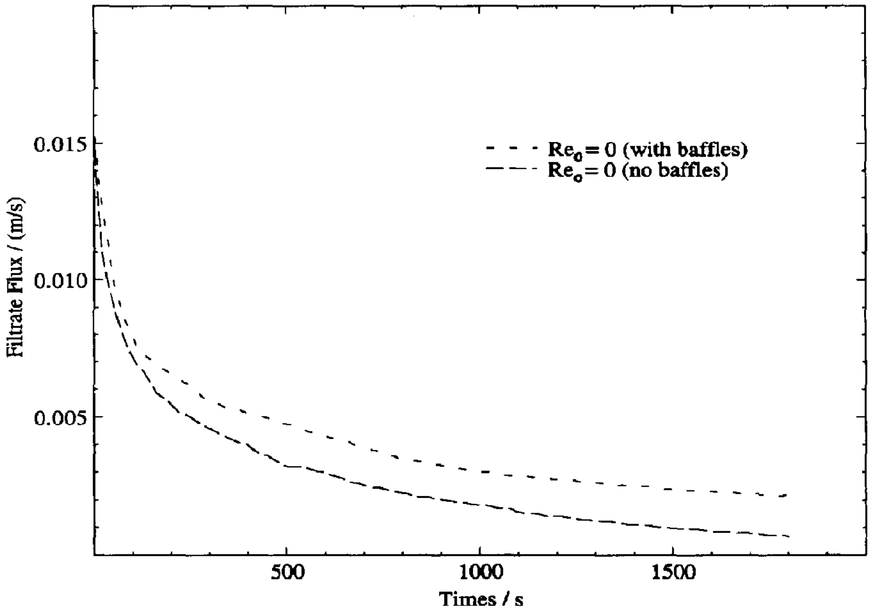

Fig. 3. Filtrate flux vs time: steady flow. $Re_n = 450$.

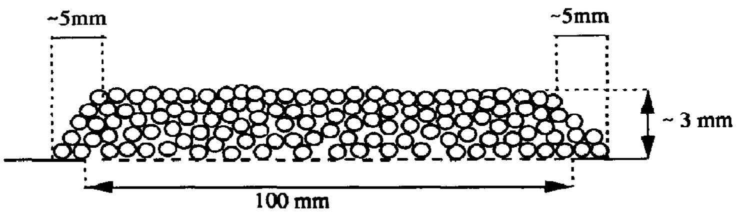

Fig. 4. Schematic diagram of a filter cake formed in steady flow.

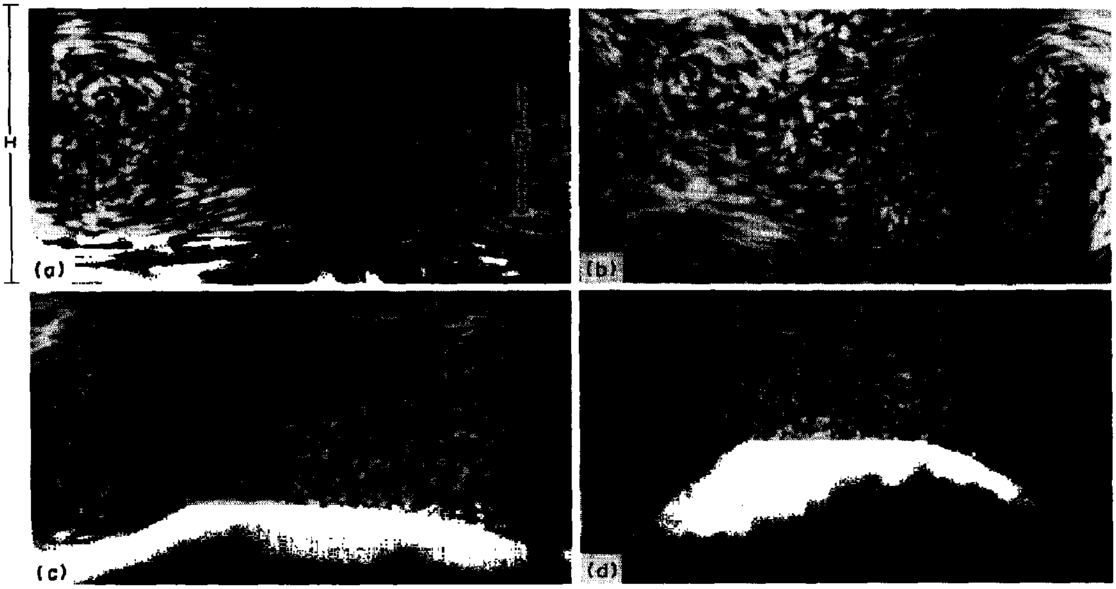

Fig. 5. Cake formation in baffled channel with steady flow, $Re_n = 450$: (a) before filtration; (b) $t = 0$; (c) $t = 500$ s; (d) $t = 1500$ s.

and B and H are the baffle and channel heights of 5 and 10 mm, respectively. It can be seen that fluid recirculation occurs downstream of the baffles and that the flow close to the filter is predominantly axial. In frame 5(b), filtration has commenced and particles are drawn with the fluid flow towards the filter surface. The fluid mechanics is altered as compared to frame 5(a) as the suspension initially flows from both up and downstream of the baffles. Frames 5(c) and 5(d) show the situation when a cake has formed. Clearly, the cake growth is significantly perturbed compared to the unbaffled channel case, with eddy circulation around the baffles causing erosion of particles from the cake. The long-term result is a shaped cake with thin sections below the baffles and a central portion of height similar to that found for the steady flow case shown in Fig. 4. Thus, it would appear that the enhancement found in filtrate flux is due to the fact that a filter cake of lower average thickness is deposited when baffles are present in the channel.

Oscillatory flow

Filtrate flux kinetics. The data obtained for filtration rate as a function of time under oscillatory flow conditions are shown in Fig. 6. A cycled sequence of filtration with and without oscillations was conducted. Initially, with oscillations applied, filtration rates are greatly enhanced compared to the steady flow results (Fig. 3) for each of the conditions shown. It can be seen that the inclusion of baffles offers a slight advantage over the unbaffled case and that a significant increase in filtrate flux is obtained when Re_0 is increased from 640 to 1280 (i.e. doubling the frequency from 5 to 10 Hz).

When the oscillations are removed (after 600 s), the filtration rates drop rapidly towards the levels obtained under steady flow conditions. It is interesting to note that the results for the baffled and unbaffled cases where Re_0 was 640, are very similar, cf the enhancement found with baffles in Fig. 1. Further, the steady flow filtrate flux for the $Re_0 = 1280$ case is higher than for the other curves, yet $Re_n = 450$ for all cases. These effects can be explained in terms of filter fouling and are discussed in more detail in the following section within the context of cake formation.

When the oscillations were reapplied, high filtration rates are regained but an overall, gradual long-term flux decline is evident. Nevertheless, significant enhancement is still found with, e.g. $Re_0 = 1280$ filtrate flux at 1500 s is about 21×10^{-3} m/s cf. $\sim 1 \times 10^{-3}$ m/s in steady flow. Also, the effect of the inclusion of baffles can be seen in that flux recovery after the quiescent period is more marked when compared to the unbaffled channel results.

Finally, during oscillatory flow filtration, gas entrainment through the filter into the channel was noted, indicating that although the overall differential pressure was essentially held constant during filtration (fluctuations due to oscillation were $< \pm 5\%$) local pressure drop fluctuations facilitated a backflush action. In order to assess the importance of this effect, experiments were conducted with the outlet chamber of the filter filled with filtrate such that a liquid environment was maintained below the filter. Figure 7 shows the filtrate flux data obtained for $Re_0 = 640$ where both oscillations and baffles were present in each case. It is clear that for this particular system, the gas entrainment is more effective than

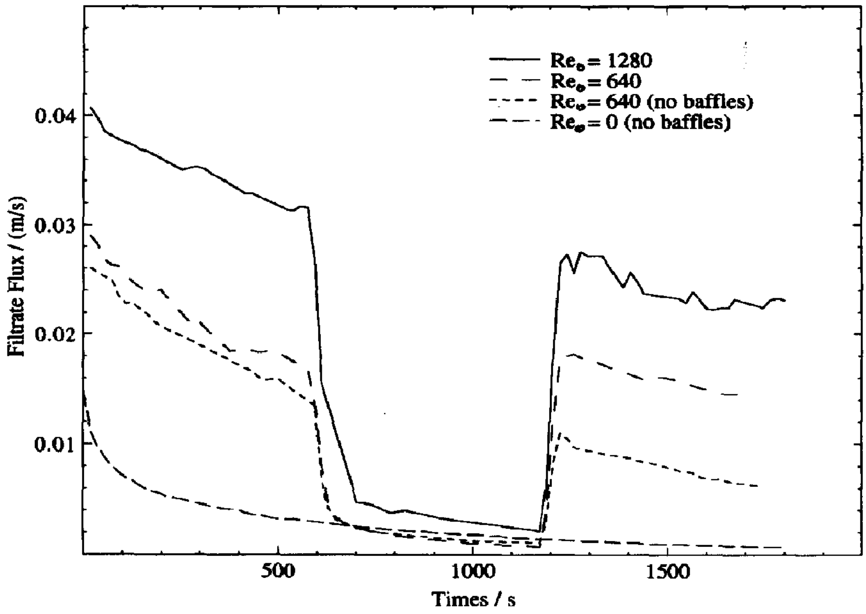

Fig. 6. Filtrate flux vs time: oscillatory flow.

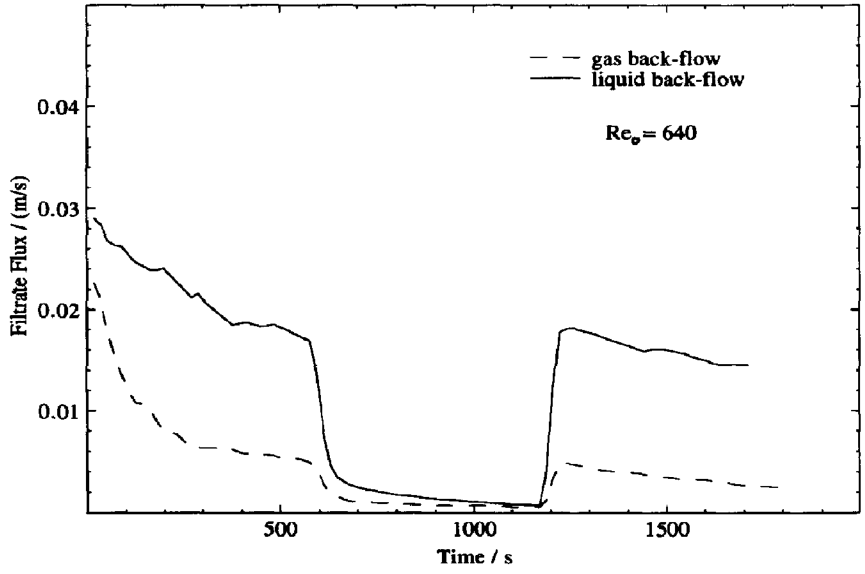

Fig. 7. Filtrate flux vs time: liquid and gas back-flow.

liquid recirculation as the filtrate flux is significantly greater in the former case, and in the latter the long-term flux is of similar magnitude to the steady flow result (Fig. 3). The effect would appear to be due to the fact that the pressure oscillations draw in a greater volume of gas than permeate because of the lower viscosity of the gas.

Cake formation. During oscillatory flow filtration, no evidence of the formation of a filter cake was observed, although, in the case where liquid recirculation was employed, a thin deposit of particles was visible on the filter when the filtration was completed. Comparison of the situations where gas entrainment or liquid recirculation occurs is facilitated by the flow visualisation photographs shown in Fig. 8, where frames (a) and (b) show gas bubble entrainment and (c) and (d) show fluid recirculation: B, H are the baffle and channel heights of 5 and 10 mm, as before. Frame 8(a), taken at flow reversal, shows the complex chaotic

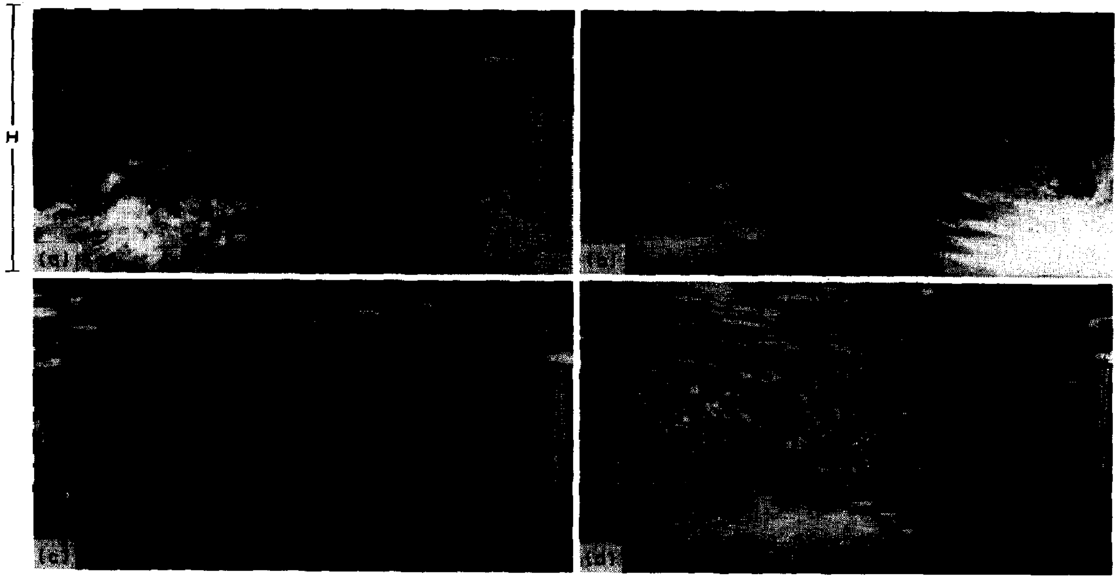

Fig. 8. Flow visualisation: (a) and (b) gas back-flow; (c) and (d) liquid back-flow.

motion of gas and particles above the filter. As the fluid accelerates from left to right in frame 8(b), a high bubble density region can be seen in the lower half of the cell, moving essentially tangential to the filter surface.

Frame 8(c) shows the situation at flow reversal for the liquid recirculation case. One dominating eddy is shed into the centre of the cell and flow at the bottom is predominantly tangential to the filter. When the flow accelerates from left to right in frame 8(d), recirculating eddies are formed downstream of the baffles and some radial motion is evident, drawing particles away from the filtration region and into the bulk fluid flow. In both frames (c) and (d), there appears to be a layer of higher particle concentration compared to the bulk close to the filter surface, which is most noticeable in frame (d) following flow reversal.

The essential differences between the gas entrainment and liquid recirculation cases are that in the former, bubbles provide an extra mechanism for fluid unsteadiness and particle removal from the filter, leading to highly chaotic mixing throughout the channel, which prevents cake build-up. With permeate back flow, a concentrated layer of particles appears to form near the filter as although fluid recirculation greatly inhibits cake build-up, radial disturbances are insufficient to draw all the particles into the bulk flow, cf. the rapidly rising bubbles in the former case. These observations would therefore appear to explain the differences in filtration rate shown in Fig. 7 and, in particular, the lack of any cake build-up would account for the greatly enhanced rates found in oscillatory mode operation compared with steady flow.

The fact that no filter cake is observed to form is however inconsistent with the gradual long-term filtrate flux decline exhibited by the data in Fig. 6. This can be explained in terms of fouling, because, although an essentially clean filter surface was observed in the gas entrainment cases, it is quite possible that particles were driven into the filter, thus blocking the pores. Certainly, evidence of particle penetration of the filter was seen in the oscillatory flow cases as particles were found in the filtrate, in contrast to the situation in steady flow. Further, it was also found that mechanical cleaning (by brushing) was required in order to restore initial rate values to their pre-oscillatory filtration level. Thus, pore blocking by particles penetrating the filter might explain long-term filtrate flux decline and the similarity between the steady flow filtration rates after oscillation in the baffled and unbaffled channel. Further, the higher steady flow rate found for the $Re_0 = 1280$ data in Fig. 6 may simply reflect a higher net removal rate of pore-blocking particles as bubble entrainment frequency was increased.

CONCLUSION

It has been found that for the cross-flow filtration of a neutrally buoyant particle suspension, fluid instabilities in the channel above the filter can greatly enhance filtrate flux. When the perturbation is caused by the introduction of periodically spaced baffles, it has been observed that the improvement is fair (approximately a factor of three) and due to erosion of the filter cake by eddies which circulate downstream of the baffles.

Under oscillatory flow conditions, the filtrate flux for this system can be increased by more than a factor of ten above the steady cross-flow value, when local differential pressure fluctuations are created which entrain gas bubbles through the filter. In this mode, the apparatus provides efficient prevention of cake build-up and operates with what is effectively a continuous back-wash. This makes it attractive compared to a cycled back-flush and it does not require retrofiltration, i.e. no filtrate has to be reintroduced to the cell. Operation using gas entrainment requires that the shell side of the filter unit does not contain liquid entirely. Our observations confirm and indeed extend those of Finnigan and Howell (1989) and Coleman and Mitchell (1991) and clearly demonstrate the viability of filtering particulate suspensions without developing a filter cake at the surface of the filter.

Acknowledgements—We would like to thank the SERC and Schlumberger Cambridge Research for funding this project.

REFERENCES

Aimar, P., Howell, J. A., Clifton, M. J. and Sanchez, V., 1991, Concentration polarisation build-up in hollow fibres: a method of measurement and its modelling in ultrafiltration. *J. Membrane Sci.* **59**, 81–99.

Brunold, C. R., Hunns, J. C. B., Mackley, M. R. and Thompson, J. W., 1989, Experimental observations on flow patterns and energy losses for oscillatory flow in ducts containing sharp edges. *Chem. Engng Sci.* **44**, 1227–1244.

Coleman, D. A. and Mitchell, W. S., 1991, Enhanced mass transfer for membrane processes. *Trans. Instn chem. Engrs* Part C, **69**, 91–96.

Colton, C. K., Henderson, L. W., Ford, C. A. and Lysaght, M. J., 1975 Kinetics of hemodiafiltration. 1. *In vitro* transport characteristics of a hollow fibre blood ultrafilter. *J. Lab. Clin. Med.* **85**, 355.

Finnigan, S. M. and Howell, J. A., 1989, The effect of pulsatile flow on ultrafiltration fluxes in a baffled tubular membrane system. *Chem. Engng Res. Des.* **67**, 278–280.

Fordham, E. J. and Ladva, H. K. J., 1989, Cross-flow filtration of bentonite suspensions. *PhysicoChemical Hydrodynamics* **11**, 411–439.

Jonsson, G., Li, W. and Johansen, P. L., 1992, Fouling of UF/MF membranes by BSA: comparison between adsorption type and pore blocking type of mechanisms, *Engng Membrane Processes*, Bavaria.

Lentsch, S., Aimar, P. and Orozco, J. L., 1992, Enhanced separation of macromolecules by combination of ultrafiltration and electrophoresis. *Engng Membrane Processes*, Bavaria.

Lu, W.-M. and Ju, S.-C., 1989, Selective particle deposition in crossflow filtration. *Sep. Sci. Technol.* **24**, 517–540.

Mackley, M. R. and Sherman, N. E., 1992, Cross-flow filtration mechanisms and kinetics. *Chem. Engng Sci.* **47**, 3067–3084.

Mackley, M. R. and Sherman, N. E., 1993, Cake filtration mechanisms in steady and unsteady flows. *J. Membrane Sci.* **77**, 113–121.

Nakao, S., Nomura, S. and Kimura, S., 1990, Transport phenomena of the cross-flow microfiltration process, In *Proceedings of Vth World Filtration Congress*, Nice, pp. 564–570.

Pearson, J. R. A. and Sherwood, J. D., 1988, Continuum modelling of cross-flow filtration, *PhysicoChemical Hydrodynamics* **10**, 647–661.

Peters, T. A. and Pederson, F. S., 1990, Memcor cross-flow microfiltration with gas back-washing: design and different applications for a new concept in *Proceedings of 5th World Filtration Congress*, Nice, pp. 473–478.

Porter, M. C., 1972a, Ultrafiltration of colloidal suspensions. *A.I.Ch. E. Symp. Ser.* **68**, 21–30

Porter, M. C., 1972b, Concentration polarisation with membrane ultrafiltration. *Ind. Engng Chem. Prod. Res. Develop.* **11**, 234–248.

Wakeman, R. J. and Tarleton, E. S., 1991a, Colloidal fouling of microfiltration membranes during the treatment of aqueous feed streams. *Desalination* **83**, 35–52.

Wakeman, R. J. and Tarleton, E. S., 1991b, An experimental study of electroacoustic cross-flow microfiltration. *Chem. Engng Res. Des.* **69**, 386–397.

Winzler, H. B. and Belfort, G., 1992, Enhanced performance for pressure-driven membrane processes: the argument for fluid instabilities. *J. Membrane Sci.* (in press).